Spatial effects define CO2 electrolysis systems

Subramanian, Siddhartha; Iglesias van Montfort, Hugo Pieter; Burdyny, Thomas

DOI
10.1016/j.checat.2024.101185

Publication date
2025

Document Version
Final published version

Published in
Chem Catalysis

Chem Catalysis

CellPress

Perspective

Spatial effects define CO_2 electrolysis systems

Siddhartha Subramanian,[1,2] Hugo-Pieter Iglesias van Montfort,[1,2] and Thomas Burdyny[1,*]
[1]Department of Chemical Engineering, Delft University of Technology, 9 van der Maasweg, 2629 HZ Delft, the Netherlands
[2]These authors contributed equally
*Correspondence: t.e.burdyny@tudelft.nl
https://doi.org/10.1016/j.checat.2024.101185

THE BIGGER PICTURE Challenges and opportunities:

- A fossil-free world is essential to prevent climate disasters but would also remove our source of carbon-based chemicals and feedstocks. Such emissions are then some of the hardest to abate and require atmospheric carbon sources to be carbon neutral at best.
- Electrochemical CO_2 electrolyzers powered by renewable energy are a potential option to replace carbon feedstocks at global scales (Mtons/year). To meet these goals, electrochemical systems must be scaled to substantial sizes.
- At scale, there will then be substantial spatial variations in reactants, products, temperature, pressure, and ionic species, complicating the scale-up and analysis of such systems. Within this perspective, we dive into the known and unknown aspects of the spatial effects that define CO_2 electrolyzers.

SUMMARY

CO_2 electrolyzers show promise as a cleaner alternative to produce value-added chemicals. In the last decade, research has shifted from classifying CO_2 reduction activity and selectivity as a catalytic property (zero-dimensional [0D]) to one that includes the complex interactions of gas, liquid, and solid species between the cathode and anode (1D). To scale CO_2 electrolyzers, however, 2D and 3D spatial variations in product selectivity, activity, and stability arise due to the design of reactor components, as well as concentration variations of the reactants, intermediates, and products. Conventional "black-box" measurement protocols are then insufficient to characterize CO_2 electrolyzers. Here, we discuss the critical multi-dimensional phenomena occurring inside these electrochemical systems, which impact the observed performance. Recent literature is used to demonstrate how a spatial perspective is essential for proper data interpretation, designing effective catalysts, and prolonging CO_2 electrolyzer lifetimes. Researchers should then define CO_2 electrolysis systems in multiple dimensions (2D and 3D).

INTRODUCTION

Low-temperature CO_2 electrolysis using renewable energy sources is an attractive route to generate fossil-free fuels and base chemicals.[1–3] After years of rapid advancements in high-performing catalysts, component integration, and efficient interface and reactor designs, the electrochemical CO_2 reduction reaction (CO_2RR) has been scaled to >100 cm^2 cells and stacks for products such as carbon monoxide, formate, acetate, and ethylene.[4–6] At the core of these developments is the use of gas-diffusion electrodes (GDEs) as catalyst supports, which are then assembled in a membrane-electrode assembly (MEA) configuration. In an MEA, the cathode, membrane, and anode are within ~0.5 mm of each other. The combination of GDEs and MEAs then enables (1) high CO_2 access to all cathode sites, allowing for current densities upwards of 200 mA cm^{-2}, (2) substantial extrinsic gains in catalytic performance through a three-dimensional (3D) porous catalyst layer, and (3) low ohmic losses, providing a pathway to full-cell voltages below 2.5 V.

A consequence of highly confined electrochemical regions and industrially viable reaction rates, however, is the formation of enormous spatial variations in CO_2, products, charge carriers, water, and temperature in the 1D direction from the cathode to the anode.[7–10] These spatial variations also extend to the 2D and 3D domains of a cell and stack, implying that the reactivity, selectivity, and efficiency of a CO_2 electrolyzer are not the same everywhere. When we upscale our systems, we then risk that the performance of our 5 cm^2 cells will not match a 100 or 1,000 cm^2 cell due to differences in local concentrations, temperature, pressure, and component stability. Such concerns extend to the different cells within a stack. Translating performance to larger scales then requires understanding the importance and sensitivity of each parameter and how they may vary spatially.

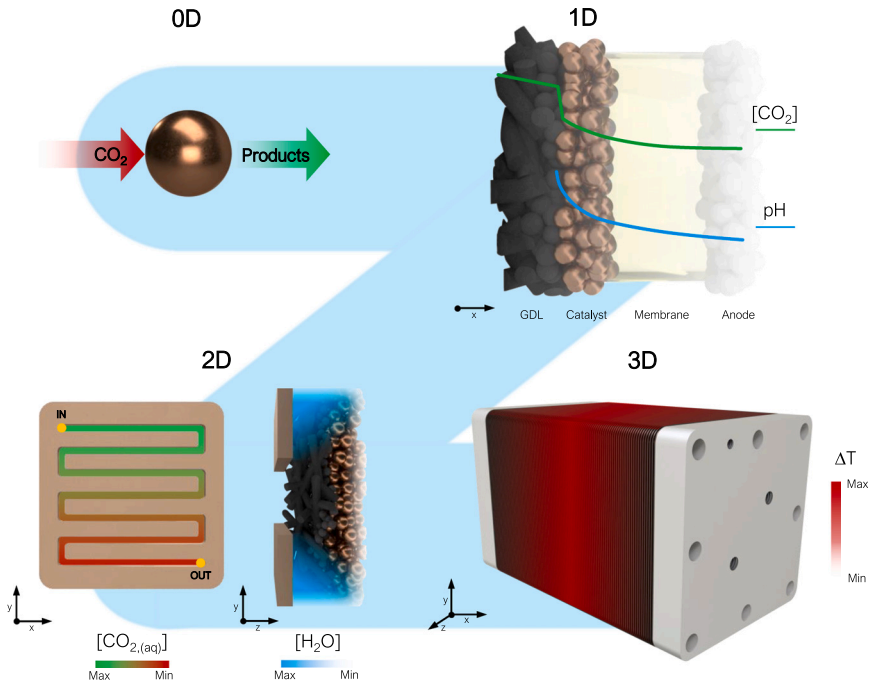

Figure 1. Study of CO_2RR electrolyzers requires a focus shift

Where in recent years, attention has been devoted to dimension-independent (0D) metrics, like Faradaic efficiencies of specific catalyst species, modeling studies have recently picked up on depth profiles of species (1D). To further advance knowledge in our field, more attention is required to be paid to 2D metrics, like special reactant distribution, and 3D aspects, like heat production and accumulation.

Notably, despite the existence of such 3D effects, the research field primarily uses 0D data to measure performance metrics.[11] Specifically, our standard electrochemical characterization techniques and gas/liquid product quantifications are almost explicitly done using inlet and outlet measurements at periodic time intervals, providing only a "black-box" perspective of a highly variable microenvironment. These "device-averaged" metrics are valuable and currently accepted in the field. Given the 3D operation of CO_2 electrolyzers (and 4D including time), however, the black-box measurement approach can lead to an incomplete understanding of the underlying behavior of our systems. The consequences of measurement uncertainty are also most pronounced in the operational domain of high CO_2 conversions, reactive products, and larger cell/stack sizes,[12,13] specifically the conditions that the fast-moving field is heading toward. An appreciation and understanding of these spatial effects and their impact on performance metrics is then needed now, combined with approaches to approximate or measure spatial effects.

In this perspective, we seek to shed light on the criticality of spatial variations in CO_2 electrolyzers, highlighting a body of recent studies employing operando techniques and multi-physics modeling tools that have identified these effects and their importance. We then provide instances where spatial effects can be used effectively to enhance performance and mitigate instability in order to increase the lifetime of an electrolyzer.

FROM 0D TO 4D EFFECTS INSIDE CO_2 ELECTROLYZERS

The electrochemical performance (activity, selectivity, efficiency, stability) of CO_2 electrolyzers is known to be governed by several factors. For example, we can tailor the performance through our choice of components. These include the type, deposition, and loading of cathode and anode catalysts, the type and dimensions of membrane/ionomers, and the choice of electrolyte and its concentration. The assembly and component configuration further plays a substantial role, as does the compression and gasketing of the system. Lastly, operating parameters such as CO_2 flow rate, temperature, pressure, current density, and voltage will directly impact our measured performance. Each of these choices by themselves alters the initial (t = 0) measurable performance. However, as electrochemical reactions occur (t > 0) and species begin to be transported throughout the system, the above factors will also separately cause an initially steady-state, open-cell environment to evolve into a temporally and spatially varying one. Within this section, we discuss spatial effects from the perspective of 0D (catalyst particle), 1D (cathode-to-anode direction), 2D (planar catalyst surface), 3D (multi-layer stack cells), and 4D (time).

At the core of our CO_2 electrolyzers is undoubtedly the atomistic catalyst surface, with the domain being roughly a nanoparticle, what we describe here as 0D from a macroscopic perspective (Figure 1A). The rate of the electrochemical CO_2RR is governed by the catalyst, applied potential, and local microenvironment surrounding the catalyst surface.[14–16] The intrinsic catalytic activity of a single catalyst particle is, in principle, determined by the turnover number (TON) and turnover frequency (TOF).[17] However, we are unable to easily characterize the activity of individual particles and precisely resolve the local electrochemical environment, meaning that we must estimate the performance through device-average metrics (e.g., current density and Faradaic efficiency [FE]) normalized by the electrochemically active surface area.[18] With precisely controlled catalyst layers (e.g., single crystals) and well-controlled conditions to more closely link observed device-averaged performances to 0D surfaces (e.g., excess CO_2 access, highly buffered solutions), many studies use *in situ* techniques. For example, online electrochemical mass spectroscopy (MS) can survey local FEs, surface-enhanced Raman and infrared spectroscopies can probe surface-bound species and near-surface concentrations for small spot sizes, and X-ray absorption spectroscopy and

neutron diffraction can identify local materials. In most cases, however, these experiments are performed in fully aqueous environments (with long CO_2 diffusion pathways) at low current densities to avoid interference from gas nucleation.

The next dimensional direction of interest is the 1D regions between the cathode and anode, which, for an MEA system, encompasses the gas-diffusion layers (GDLs) and microporous layers, catalyst layer, ion-exchange membrane, anode, and anolyte (Figure 1B). This region, constituting less than 1 mm in distance, has extremely high variations in concentrations of CO_2, products, ions, and water, as evidenced through continuum transport modeling and observed experimental effects such as flooding and salt precipitation.[8,9,19] A deep understanding of the transport phenomena of this region has directly led to the development of new anion-exchange membranes (AEMs; e.g., Sustainion, PiperION), the use of Cs+ as a cation, the lowering of anolyte concentrations, appropriate catalyst deposition procedures, and optimum cell compression.[20,21] While much greater detail can be discussed regarding the critical 1D domain, these considerations are well accepted in the research field and covered elsewhere. For this perspective, we then put greater emphasis on the 2D-3D spatial effects (Figures 1C and 1D), which are more underexplored but critical for scale-up efforts of the technology.

Zooming out from the dominant 1D profile, we can consider a large variety of 2D planes. The 2D plane of most spatial importance and performance criticality, however, is assuredly the in-plane dimension of an individual cell that is perpendicular to the aforementioned 1D region. Slices of this region include the CO_2 gas channel, GDE, catalyst layer, membrane, and anode. For example, in the anode compartment, a pure liquid anolyte typically enters a cell, but this quickly becomes a two-phase mixture of anolyte and CO_2/O_2 gas as products evolve and carbonate crosses over the membrane. Near the latter part of the cell, these gases can block active sites on the anode, as well as spatially influence the ohmic drops within a system. Combined, the anode effects can then cause the CO_2RR's local current densities and electrode potentials to vary, which impact the observed performance metrics. In small cell research, we then typically overflow the anolyte (e.g., 20 mL min^{-1} for a 5 cm^2 anolyte) to avoid high gas-to-volume ratio (e.g., void fraction) issues and boost performance. However, at very large cell areas, pressure drops and pumping work become important considerations, and excess anolyte flow may not be a viable option. To aid in predicting behavior at various scales, we then use traditional chemical engineering non-dimensional relationships to determine required system pressures and flow rates to avoid challenges such as high void fractions in the anolyte channel.

We would like to center most of our discussion, however, on the CO_2 gas channel, GDL, and catalyst layer spatial variations, as there are clear reports of how spatial effects impact the measured performance metrics. Within these three components from the inlet to the outlet of the reactor, we have CO_2 being consumed and products being produced, resulting in a concentration gradient across a singular cell. Additionally, our systems use flow fields of various patterns to supply gas, remove products, and compress cells together, all of which add additional spatial complexities. Here, we briefly discuss three dominant spatial considerations of the 2D planes of the cathodic side.

Firstly, due to CO_2 and product gradients across even small 5 cm^2 cells, the cathodic FE can vary greatly from the inlet to the outlet of the reactor, particularly for CO_2 λ values (also called CO_2 excess) of 2–5. Such local FE values were first shown in our work for CO_2 to CO on a silver (Ag) catalyst, where we noticed through 2D modeling that there were regions of the catalyst layer that were depleted of CO_2, even though the gas channel still contained abundant reactant.[13] In this work, we discuss the implications of local FEs versus device-averaged FEs. We then followed up this work by utilizing different flow-field patterns (FFPs), which showed even greater spatial variations in concentrations, and discussing resistance to blockages of different FFPs due to single versus multiple gas pathways.[22] Recently, further considerations were applied for a copper (Cu) catalyst, where the residence time of intermediate CO was considered.[23] Here, we showed that the concentration and amount of time that CO resides in the catalyst layer is influenced by both CO_2 flow rates and the utilized flow fields. Lastly, in a case of direct CO electrolysis, Simonson et al. measured FEs at different locations using a copper electrode and a segmented cell reactor.[24] Here, spatial differences in ethylene and H_2 partial current densities were observed at various inlet flow rates and CO partial pressures. Collectively, these examples provide the motivation to contrast 2D FEs versus 0D measured FEs to sufficiently characterize the phenomena happening within systems.

A second conclusion resulting from acknowledging 2D concentration gradients across the gas channel is that there can be selectivity benefits by varying the composition of the catalyst layer spatially, which in turn can tune CO_2/CO ratios and shift C_{2+} production. This strategy has been widely shown in a number of studies employing tandem Ag/Cu or Zn/Cu catalyst systems to tune CO coverage and enhance C_{2+} or oxygenate production.[25–27] For instance, Zhang et al. designed a Cu/Ag segmented GDE (s-GDE) and found that a CO-selective catalyst near the inlet (Ag) of the reactor and a Cu catalyst at subsequent segments maximizes C_{2+} partial current densities to >1 A/cm^2.[28] The strategy of controlling the spatial management of by-products like CO shows how having a spatial perspective of electrochemical systems can be beneficial in designing effective catalyst layers for enhanced product formation rates.

A third 2D factor to consider on the cathode side is the water management. Too much or too little water in the membrane, catalyst layer, and GDE is problematic. Here, we must admit that there is still plenty to understand regarding water transport in CO_2 electrolysis systems, with both salt precipitation and flooding common occurrences in experimental testing. Within a CO_2 electrolysis system, water can be supplied and taken away from the cathode through the CO_2 gas stream, as well as by transport through the membrane. In an early work on humidification, Wheeler et al. showed that the water concentration at the catalyst-membrane interface remained constant in an MEA electrolyzer employing an Ag catalyst, and humidity at the cathode feed was found to affect the production of CO significantly.[29] Using humidity sensors in the reactor and a numerical transport model, they showed that humidity at the cathode inlet feed modulated the flux of water transport and potassium cation

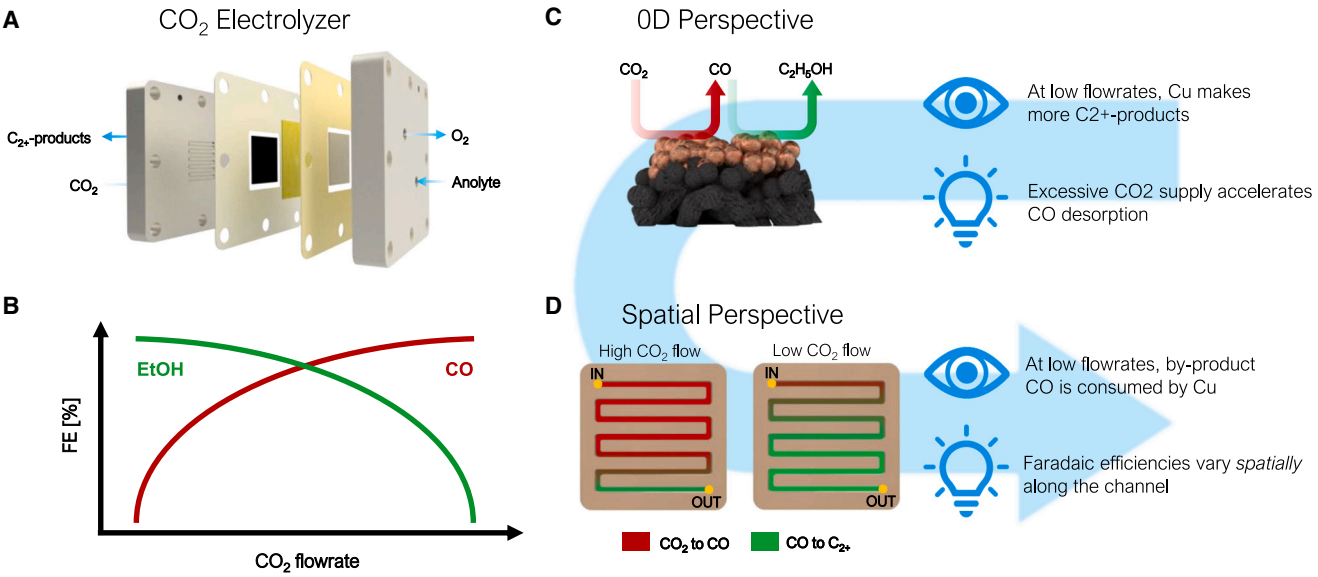

Figure 2. A spatial perspective on phenomena observed during operation sheds new light on the complexity of CO_2RR electrolyzers

(A) In a zero-gap MEA, the cathode evolves CO_2 and water to, e.g., C_{2+} products.

(B) A common effect observed in these electrolyzers is the shift in selectivity from ethanol to CO at higher flow rates.

(C) If we read this observation as independent of space coordinates, then we can be tempted to couple selectivity with convection effects.

(D) The reality is, however, that flow rates change the concentration of species in an unequal way along the channel, as do selectivities.

crossover from the anode to cathode. These works have also been contrasted by Choi et al., who emphasize a net water flux from the anode.[30] Probing directly into the GDE and catalyst layer, the work by Disch et al. showed the complex variations in hydration using neutron imaging. Specifically, large water content differences were observed in a flow field's land versus channel areas, at least in part due to differences in the compression of the GDE and the preferential evaporation of water from the channel areas.[31] Due to the flow field both supplying gases and providing cell compression, large water differences were found between the two regions. This specific example is discussed more in the next section. Overall, water management in MEA reactors is important due to two common failure mechanisms: flooding of the carbon GDE and (bi)carbonate precipitation at the cathode. A proper understanding of water management and the associated trade-offs in water concentrations at the cathode side is then essential for improving the lifetime of these electrolyzers. In addition to concentrations of reactants (CO_2, H_2O), it is important to emphasize here that variations in the concentrations of ions (K^+, OH^-, HCO_3^-, and CO_3^{2-}) at the catalyst microenvironment also alter reaction rates. For example, a higher local cation concentration around the catalyst surface is known to increase C-C coupling and C_{2+} product formation rates in Cu-based MEA reactors in both alkaline and acidic conditions.

To illustrate how spatial dimensions can lead to differing hypotheses, we take the CO_2RR on a copper (Cu) catalyst as an example (see Figure 2). We see from this figure that Cu produces the highest FE toward C_{2+} products and the lowest FE toward CO at lower inlet CO_2 flow rates. Since CO is the intermediate for the formation of C_{2+} products, interpreting this from a 0D perspective (as shown in Figure 1A) might lead to a possible conclusion that an excessive CO_2 supply reduces C-C coupling due to competition between *CO desorption and CO-CO coupling.[32] For example, a previous study by Robert et al. showed that adsorbate-adsorbate repulsion on Cu can facilitate *CO desorption and CO evolution.[33] In contrast, taking a spatial perspective might reveal an alternate hypothesis of a higher reactant residence time inside the electrolyzer (GDE and gas channel) as an alternate explanation for the observed increases in C_{2+} selectivity at lower flow rates. This means that as electrolyzers are scaled up (>1 cm^2), spatial FE distributions arise inside the reactor, with the regions near the inlet feed predominantly producing CO_2-to-CO and those down the channel producing CO-to-C_{2+} products (see Figure 2). It is important to understand these spatial differences, as any variation will further be amplified when electrolyzers are scaled up.

For 3D systems, we primarily think of an electrolyzer containing multiple cells within a larger stack. There are then considerations of how to feed CO_2 into all the cells to prevent transport issues, as well as ensuring that each cell within a stack performs similarly or close to their optimal conditions. While assembly and design (e.g., gas headers, sealing, parallel/series power supply, shunt currents, etc.) are critical factors for having a well-functioning stack, there will still be spatial variations that can impact behavior. A clear example of this is spatial temperature and pressure variations that will be unavoidable as a result of heat evolution and gas evolution, respectively. Controlling for these factors is needed as we move to large cell areas and numbers of cells that are typically only powered in a singular series connection. The current then flows through each cell equally, while the voltage requirements of each cell can differ. Means of in-line temperature

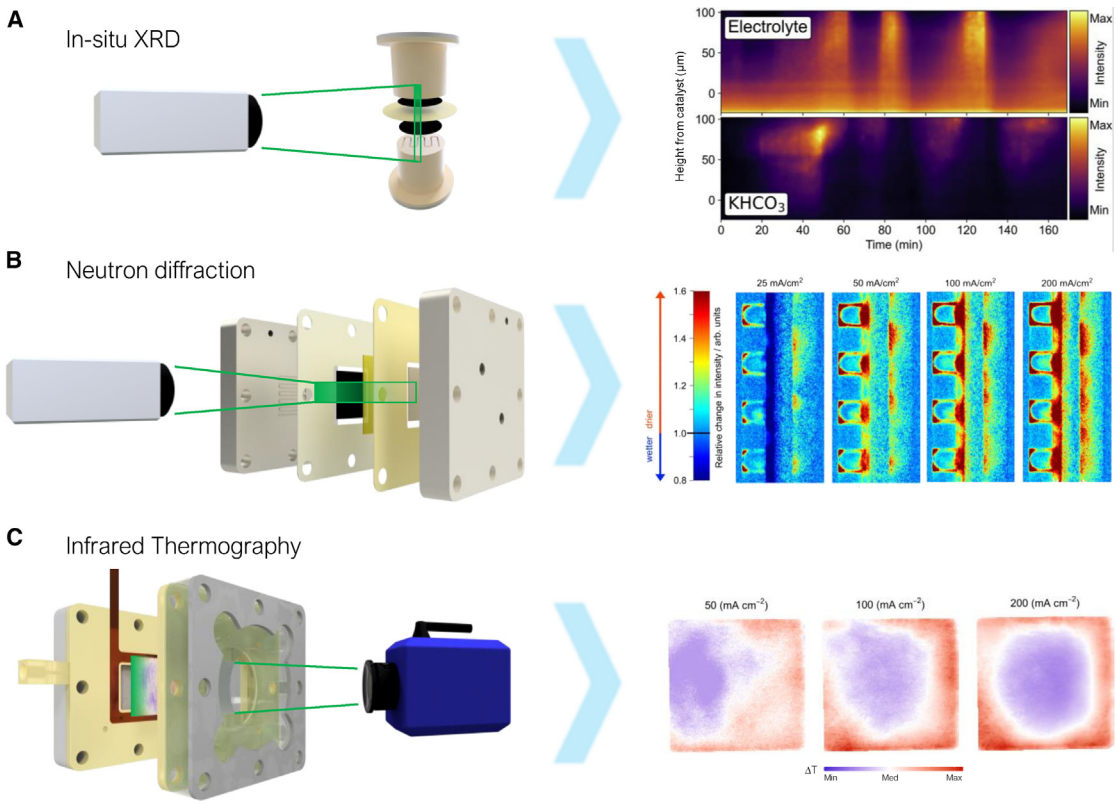

Figure 3. Recent developments in the field have enabled 2D visualization of phenomena occurring in CO_2RR electrolyzers

(A) *In situ* XRD reveals the species dynamics in and around the catalyst layer of an MEA (adapted from Moss et al.[35] under a CC BY 4.0 license, copyright 2023 Elsevier B.V.).

(B) A neutron diffraction analysis enables visualization of accumulation of water and salts between the membrane and cathode at relevant current densities (adapted from Disch et al.[31] under a CC BY 4.0 license, copyright 2022 Springer Nature Group).

(C) Infrared imaging of the cathode's backbone is a valid proxy for activity distribution of the catalyst in an x-y plane (adapted from Iglesias van Montfort et al.[38] under a CC BY 4.0 license, copyright 2023 Springer Nature Group).

management and system control by varying ramp rates and fluid flow are then ways of ensuring optimal and stable performance, emphasizing the necessity of 4D considerations if we begin to commercialize these technologies.

OPERANDO VISUALIZATION AND MODELING OF SPATIAL EFFECTS

While spatial variations can be inferred from black-box data and numerical models or probed with in-cell measurement points using humidity sensors or in-channel product quantification, these approaches still approximate or infer spatial effects. Direct measurement of spatial effects both in-plane and through the catalyst layer remains essential.[34] Here, operando techniques such as *in situ* X-ray diffraction (XRD), neutron diffraction, Raman spectroscopy, and infrared thermography have just begun to probe CO_2 electrolyzers, despite their usage in adjacent electrochemical fields. These techniques are often already in use by the field to study catalysts in a 0D fashion but can thus easily be repurposed to study spatial effects in an electrolyzer. Here, we will discuss some of these techniques and encourage their adopted use.

As an example of the application of such techniques, Moss et al. used *in situ* XRD studies of a Cu-based AEM electrolyzer held at a constant current. Here, they observed the formation of bicarbonate salts over time within the GDE. These precipitated salts blocked active sites on the catalyst for the CO_2RR and, subsequently, caused a decline in the FEs of the products. Interestingly, though, the authors observed this decline in the FEs of CO_2RRs to be temporary, and during the increase in hydrogen evolution, excess water caused the bicarbonate salts to dissolve, reopening CO_2 access to the catalyst and again increasing CO_2RR FEs. A constant drop and rise of FEs was observed over fixed intervals, resulting in an oscillatory decline in the FEs of CO_2RRs (Figure 3A).[35] This same technique also served to show the influence of alkali cation effects on the precipitation of carbonates and flooding in GDEs.[36] These results not only provide insights into the flooding of the GDE and the subsequent decline in performance but also help to understand ion transport mechanisms in AEMs under CO_2RR conditions, which are beneficial for designing AEMs specifically suited for CO_2 electrolyzers. Disch et al. used the neutron diffraction technique in a zero-gap MEA reactor and revealed that areas under the rib/land regions showed higher CO_2RR activity than at the gas flow-field regions due to higher

water concentrations at the rib regions (Figure 3B).[37] Considering that the gas flows in the gas channels at the back of the GDE, it is likely that these channels are drier than the rib regions. This means that higher the water concentration under the rib regions enables lower rates of salting-out effects as compared to the channel regions. Additionally, our previous work on the influence of the gas FFP on CO production showed that a higher pressure drop at the cathode side generated by a serpentine flow pattern resists electrolyte flooding the GDE, prolonging the lifetime of the electrolyzer.[22] The design of proper gas flow-field designs, rib spacing, and humidification are then crucial considerations for the development of stable CO_2 electrolyzers.

In addition to these spatial variation in species concentrations, proper quantification of pH gradients around the catalyst-coated GDL are essential, as the competing hydrogen evolution reaction (HER) and products like CH_4 are known to be pH dependent, as well as CO_2 utilization and deposition of carbonates on the catalyst layer. This is where 1D reaction diffusion models have greatly enabled researchers to estimate pH gradients at various operating conditions and reactor configurations.[7,39–41] A few studies have used operando techniques to estimate pH gradients around the catalyst surface in GDE flow cells in a 2D manner. A study by Lu et al. using operando Raman spectroscopy in a GDE flow cell showed the direct observation of pH gradients, and the results were in good agreement with their reaction diffusion models.[42] For example, a similar study by Böhme et al. showed maps of local pOH around the catalyst surface using confocal laser scanning microscopy (CLSM) and observed a higher pH in the microtrenches of the GDE.[43] While each of these techniques comes with its own advantages and limitations in terms of cell design and spatial resolution in space and time, we posit that combining experimental measurements with reaction diffusion modeling can allow for greater conclusions to be made. This is particularly the case for techniques like CLSM, where the depth and distancing from the catalyst can be better resolved by varying focal depth.

Additional means of probing local electrochemical activity are, for example, through infrared thermography (Figure 3C), where thermal responses in time are a proportional result of electrochemical activity. In our previous work, we used infrared thermography to probe the local heat generated in a catalyst-coated GDL during operation under various conditions.[38,44] At higher current densities during CO_2RRs at ambient temperature, we found an Ag catalyst to be >10 K hotter than the comparable electrolyte temperature. Such an observation has implications for modeling and kinetic studies whose properties (CO_2 solubility, reaction rates, diffusion, etc.) are strongly tied to temperature. As industrial CO_2 electrolyzers are likely to be operated at much higher current densities, it is important to understand that catalyst, during operation, might be significantly hotter than the electrolyzer itself. Once again, this study shows why considering electrochemical reactions in multiple dimensions is beneficial for proper data interpretation and understanding of the phenomena occurring inside the electrolyzer.

LOOKING FURTHER: THE GDE AS A 3D REGION

An important realization, in addition to the variation of the nature of catalyst in the 2D plane, is the intrinsic complexity of the catalyst layer in the third dimension. The plethora of deposition methods reported in the literature result in an equally complex landscape of electrode topologies. In a system that is very sensitive to local concentration of reactants,[45] tortuosity of the fluid phase,[46] and basicity,[47] this leads to a blurred understanding of the observed effects at play during CO_2RRs. For added complexity, some catalysts, like copper, show an inherent instability that results in shifting product selectivities in time. These issues highlight the importance of understanding the role of our catalyst layer in the reaction system and the influence the deposition technique has on the performance metrics.

In a drive to tackle the instability of some catalysts, it can be enticing to "overload" the electrode with active particles. This prevents the catalyst activity from being a bottleneck in benchtop tests in a lab environment. Since catalyst loading is often overlooked as a variable in electrode development for CO_2RRs, this practice goes mostly unnoticed. If one imagines a catalyst layer as a region with a progressively deactivating regime, a thicker catalyst layer benefits the stability of the system overall. This comes at a cost of a thicker catalyst layer, but the reduced increase in this dimension relative to the overall cathode size seems a valid compromise. For context, Cu catalysts are diverse in the literature, and reported loadings are in the range of 0.1–3 mg cm^{-2}, spanning two orders of magnitude.[48–63] The main impacts of this practice are, for one, a skewed representation of the partial current density toward a certain product, and two, misleading reporting on the stability of the catalyst, as the active region may be allowed to progress through the layer during the experiments.

The problem of this blind spot in literature comes when constant-potential tests are performed. Two electrodes with the same active catalyst but dissimilar loadings will display different current densities when subjected to the same polarization. The reason for this is simply that there are more electrochemically active sites per unit area (Figures 4A and 4B). In addition, the common practice in the CO_2RR field is to condense current densities to a 2D geometric area, disregarding the active electrochemical surface area. This draws unrealistic performance metrics of the catalytic materials by ignoring the third depth dimension in electrode development. A richly loaded catalyst layer allows for an appropriate level of activity at the gas-liquid interface, where gaseous CO_2 dissolves into the electrolyte phase and then reacts at the catalyst surface (Figure 4C).[45] Deeper into the catalyst layer, CO_2 availability decreases due to consumption and longer diffusion distances, leading to variable CO_2RR activity through the catalyst layer. Conversely, by operating at lower current densities, CO_2 penetration increases, and more material can be used to facilitate the reaction. Thus, even if catalyst layers deactivate over time, there is ample material to continue reacting (Figure 4D).[64]

As a separate issue, catalyst layer thickness directly impacts the local availability and penetration depth of aqueous CO_2. While CO_2 solubility is generally high enough for industrially relevant current densities,[40] this metric is considerably affected by environmental factors like the presence of ions, temperature, and pressure of the gas phase.[65,66] CO_2 availability and average concentration in the aqueous phase of a thin catalyst layer of, say, 50 nm is then much more uniform than that of a 5 μm

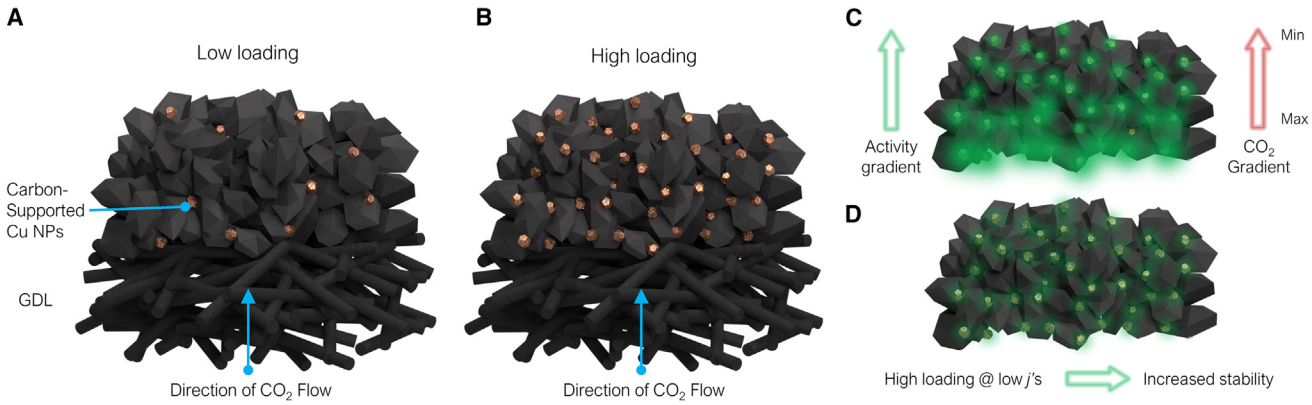

Figure 4. Catalyst loading directly affects the performance metrics of a CO_2RR GDE

(A) Sketch of the proximity of the catalyst layer in a low-loading GDE.

(B) Same sketch for a high-catalyst-loaded GDE.

(C) A high loading enables a high presence of active species at the regions with highest CO_2 concentrations.

(D) During stability tests, GDEs with a high loading show increased stability.

catalyst layer.[48,67] This phenomenon is even more influential considering the dependance of certain catalysts like copper to the local ratio between reactant CO_2 and other intermediates like CO.[68] Furthermore, the tortuosity and complex structure of the active region of the GDE might result in varying pH conditions: a region with less convective or diffusive transport will result in the accumulation of carbonate species. Besides affecting the structural integrity of the catalyst,[69] this can result in a shift in the product selectivities.

The ideal catalyst layer thickness is then subject to different contrasting constraints. On one side, higher current densities would benefit from greater catalytic surface areas to boost activity extrinsically. However, higher current densities limit the penetration depth of CO_2, and excess material only limits ion/water transport while acting as a hydrogen evolution catalyst. The ideal catalyst layer is then likely one that is current density dependent or facilitates CO_2 throughout the entire depth.

Considering the historical influence of water electrolysis and fuel cell fields in CO_2RR literature, it is striking that most spatially resolved analysis techniques remain unexplored for this application. While tomography is beginning to make an appearance as an imaging technique for 2D variations in time,[70–72] using this technique to back-relate observations to hypotheses is still far from mature. Efforts from electrolyzer and fuel cell studies have, in this regard, led to abundant modeling resources that could easily be translated toward efforts for CO_2RRs.[73,74]

CURRENT DENSITY DISTRIBUTION IN GDEs

An often overlooked spatial variability in GDEs is current density across the catalyst layer.[38] Typically voltage from a power source is provided to cables which proceeds through a current collector (e.g., a metal flow field or copper tape), then the GDL and into the catalyst layer. However, current flowing through any substrate will encounter resistance and potential loss. As a current collector typically plays a dual role as gas distributor, current passing into the catalyst layer must go laterally through the GDL in some places. While carbon GDLs are considered to be sufficiently conductive, they are far from perfect conductors, and potential variations occur even over short distances. As larger electrodes are examined, current collection distances should then not be scaled with the cell area but rather maintained similar to current 1–5 cm^2 cells (e.g., 1 mm). Otherwise, the conductivity of carbonous supports will be challenged, leading to spatial voltage and current density variations across the electrode.[75–77] These issues are further compounded for alternative GDL materials like expanded polytetrafluoroethylene (ePTFE), which is non-conductive and requires current distribution primarily through the catalyst layer itself.

Carbonous electrodes have a long-standing history of usage in the CO_2RR field, as their conductive backbone provides a solid base of conductivity and porosity and (combined with hydrophobic particles) an acceptable resistance to flooding. The latter, however, has been increasingly put under pressure as reports of flooding and its limited resistance to the CO_2RR surfaced.[31] For example, in our previous work, we showed that under potentials more cathodic than −0.65 versus a reversible hydrogen electrode, the microporous layer of a GDL will become more hydrophilic and allow flooding to occur.[78] A flooded carbon GDL then results in greater CO_2 diffusion distances to the catalyst layer, increasing mass-transfer resistance.[38] A portion of the GDE at high potential, then, experiences more rapid flooding and, thus, a reduction in selectivity toward CO_2 products than a relatively drier portion. Imaging of these phenomena, especially that of the spatial distribution of flooding, is a valuable proxy to study current distributions.

In this regard, it may be attractive for the field of CO_2RRs to collect the current at the posterior side of the catalyst—that is, using a front-contact current collector. This ensures that the variability of the collected current is not dependent on the gas-channel design and opens up the opportunity to design a spatially variable current density to match local reactant conditions. This also relieves the carbonous back layer of any variations in local potential or current density so that flooding does not become an interface problem. Alternatively, a less-conducting

GDL might be compensated for by a robust anterior current collection system, for example, using flexible nickel meshes.[79]

A different strategy to avoid microporous flooding involves using super-hydrophobic MPLs insensitive to the interface potential. The most widespread application of this is the appearance of ePTFE GDEs in the CO_2RR field. These PTFE meshes avoid macroscopic flooding by the intrinsic properties of the polymer, with the obvious caveat that they are non-conductive. This means that every form of current collection must proceed through the front, active part of the electrode in an in-plane geometry. Supplying electrons in this manner greatly strains the conductivity of the electrode and induces great current distribution inequalities, especially for thin catalyst layers.[38] Different strategies to tackle this have been proposed, from a non-active graphitic sandwich layer,[48] to woven current collecting wires,[80] to insulated conductive plates[81] and non-invasive busbar electrodes.[38] The challenge for this architecture, overall, lies in engineering a technique that is scalable to industrial, meter-scale electrodes.

The observations in this section are again in stark contrast with developments in the water electrolysis and fuel cell fields, where the analysis of current distributions through the usage of so-called segmented cells has a long-standing history.[76,82–85] The implementation of such technology leads, in our perspective, to the rapid standardization of designs for testing, enabling a fairer comparison of performances between different solutions to the current distribution.

TEMPORAL EFFECTS IN CO_2 ELECTROLYZERS

While much of the discussion so far has centered around 1D, 2D, and 3D spatial effects, additional changes related to time can also occur in the electrolyzer. For example, morphological changes of the anode/cathode catalysts are often observed during electrolysis, which could, in a few instances, cause performance deterioration over time. However, these changes are generally not expected to significantly affect performance, as maintaining steady-state operation of a CO_2 electrolyzer is often desirable for long-term stability. One of such changes that has been reported in an AEM-based CO_2 electrolyzer at practical operating conditions is the stability of the anode catalyst. IrO_2 is usually the popular choice of anode catalyst for water oxidation reactions at the anode side, and degradation rates in the cell potential of 10–50 μV/h are usually reported due to catalyst leaching from the platinized titanium support.[86] To alleviate this issue, it is important to optimize the catalyst loading, ionomer/solvent ratio during catalyst ink preparation as well as follow proper protocols for catalyst coated membrane (CCM) preparation in zero gap CO_2 electrolyzers. Further, monitoring the leaching of such components during operation using advanced characterization techniques such as x-ray absorption spectroscopy (XAS) and inductively coupled plasma-MS (ICP-MS) will be essential to ensure a stable long-term operation (>1,000 h), much required for practical applications.

CONCLUSIONS

The vast array of overlapping phenomena occurring in CO_2 electrolyzers will make it an interesting research field for years to come. For the technology to be reliably scaled further, however, greater efforts are required to understand and optimize the 2D, 3D, and 4D effects occurring in CO_2RRs. Without such an appreciation, we are likely to continuously run into bottlenecks that then need to be solved on a case-by-case basis. Here, traditional chemical engineering scaling principles should be applied to electrochemical systems to foresee problems ahead of time, which requires a mixture of older and newer sensing techniques on multiple dimensions. We hope that this perspective provides a basis for the multi-dimensional effects occurring and spurs innovations as researchers and industry attempt to scale CO_2RRs.

RESOURCE AVAILABILITY

Lead contact

Further information and requests should be directed to the lead contact, Thomas Burdyny (t.e.burdyny@tudelft.nl).

Materials availability

All materials are contained in the main text.

Data and code availability

There is no code or data in this perspective.

ACKNOWLEDGMENTS

H.-P.I.v.M., S.S., and T.B. would like to acknowledge the co-financing provided for this project in the context of the e-Refinery Institute by Shell Global Solutions International B.V. and the Top Consortia for Knowledge and Innovation (TKI) of the Dutch Ministry of Economic Affairs.

AUTHOR CONTRIBUTIONS

Conceptualization, H.-P.I.v.M. and S.S.; methodology, S.S., H.-P.I.v.M., and T.B.; investigation, S.S. and H.-P.I.v.M.; visualization, H.-P.I.v.M., S.S., and T.B.; funding acquisition, T.B.; project administration, T.B.; supervision, T.B.; writing – original draft, S.S. and H.-P.I.v.M.; writing – review & editing, S.S., H.-P.I.v.M., and T.B.

DECLARATION OF INTERESTS

The authors declare no competing interests.

SUPPLEMENTAL INFORMATION

Supplemental information can be found online at https://doi.org/10.1016/j.checat.2024.101185.

REFERENCES

1. Wakerley, D., Lamaison, S., Wicks, J., Clemens, A., Feaster, J., Corral, D., Jaffer, S.A., Sarkar, A., Fontecave, M., Duoss, E.B., et al. (2022). Gas diffusion electrodes, reactor designs and key metrics of low-temperature CO2 electrolysers. Nat. Energy *7*, 130–143. https://doi.org/10.1038/s41560-021-00973-9.
2. Masel, R.I., Liu, Z., Yang, H., Kaczur, J.J., Carrillo, D., Ren, S., Salvatore, D., and Berlinguette, C.P. (2021). An industrial perspective on catalysts for low-temperature CO2 electrolysis. Nat. Nanotechnol. *16*, 118–128. https://doi.org/10.1038/s41565-020-00823-x.
3. Küngas, R. (2020). Review—Electrochemical CO $_2$ Reduction for CO Production: Comparison of Low- and High-Temperature Electrolysis Technologies. J. Electrochem. Soc. *167*, 044508. https://doi.org/10.1149/1945-7111/ab7099.

4. Endrődi, B., Kecsenovity, E., Samu, A., Darvas, F., Jones, R.V., Török, V., Danyi, A., and Janáky, C. (2019). Multilayer Electrolyzer Stack Converts Carbon Dioxide to Gas Products at High Pressure with High Efficiency. ACS Energy Lett. *4*, 1770–1777. https://doi.org/10.1021/acsenergylett.9b01142.

5. Lee, W.H., Lim, C., Lee, S.Y., Chae, K.H., Choi, C.H., Lee, U., Min, B.K., Hwang, Y.J., and Oh, H.-S. (2021). Highly selective and stackable electrode design for gaseous CO2 electroreduction to ethylene in a zero-gap configuration. Nano Energy *84*, 105859. https://doi.org/10.1016/j.nanoen.2021.105859.

6. Wei, P., Gao, D., Liu, T., Li, H., Sang, J., Wang, C., Cai, R., Wang, G., and Bao, X. (2023). Coverage-driven selectivity switch from ethylene to acetate in high-rate CO2/CO electrolysis. Nat. Nanotechnol. *18*, 299–306. https://doi.org/10.1038/s41565-022-01286-y.

7. Weng, L.-C., Bell, A.T., and Weber, A.Z. (2018). Modeling gas-diffusion electrodes for CO_2 reduction. Phys. Chem. Chem. Phys. *20*, 16973–16984. https://doi.org/10.1039/C8CP01319E.

8. Weng, L.C., Bell, A.T., and Weber, A.Z. (2019). Towards membrane-electrode assembly systems for CO2 reduction: A modeling study. Energy Environ. Sci. *12*, 1950–1968. https://doi.org/10.1039/c9ee00909d.

9. Weng, L.-C., Bell, A.T., and Weber, A.Z. (2020). A systematic analysis of Cu-based membrane-electrode assemblies for CO_2 reduction through multiphysics simulation. Energy Environ. Sci. *13*, 3592–3606. https://doi.org/10.1039/D0EE01604G.

10. Agliuzza, M., Pirri, C.F., and Sacco, A. (2024). A comprehensive modeling for the CO_2 electroreduction to CO. JPhys Energy *6*, 015004. https://doi.org/10.1088/2515-7655/ad0a39.

11. Iglesias Van Montfort, H.-P., Subramanian, S., Irtem, E., Sassenburg, M., Li, M., Kok, J., Middelkoop, J., and Burdyny, T. (2023). An Advanced Guide to Assembly and Operation of CO_2 Electrolyzers. ACS Energy Lett. *8*, 4156–4161. https://doi.org/10.1021/acsenergylett.3c01561.

12. Kas, R., Star, A.G., Yang, K., Van Cleve, T., Neyerlin, K.C., and Smith, W.A. (2021). Along the Channel Gradients Impact on the Spatioactivity of Gas Diffusion Electrodes at High Conversions during CO2 Electroreduction. ACS Sustain. Chem. Eng. *9*, 1286–1296. https://doi.org/10.1021/acssuschemeng.0c07694.

13. Subramanian, S., Middelkoop, J., and Burdyny, T. (2021). Spatial reactant distribution in CO_2 electrolysis: balancing CO_2 utilization and faradaic efficiency. Sustain. Energy Fuels *5*, 6040–6048. https://doi.org/10.1039/D1SE01534F.

14. Nitopi, S., Bertheussen, E., Scott, S.B., Liu, X., Engstfeld, A.K., Horch, S., Seger, B., Stephens, I.E.L., Chan, K., Hahn, C., et al. (2019). Progress and Perspectives of Electrochemical CO2 Reduction on Copper in Aqueous Electrolyte. Chem. Rev. *119*, 7610–7672. https://doi.org/10.1021/acs.chemrev.8b00705.

15. Nwabara, U.O., Cofell, E.R., Verma, S., Negro, E., and Kenis, P.J.A. (2020). Durable Cathodes and Electrolyzers for the Efficient Aqueous Electrochemical Reduction of CO_2. ChemSusChem *13*, 855–875. https://doi.org/10.1002/cssc.201902933.

16. Stephens, I.E.L., Chan, K., Bagger, A., Boettcher, S.W., Bonin, J., Boutin, E., Buckley, A.K., Buonsanti, R., Cave, E.R., Chang, X., et al. (2022). 2022 roadmap on low temperature electrochemical CO_2 reduction. JPhys Energy *4*, 042003. https://doi.org/10.1088/2515-7655/ac7823.

17. Kutz, R.B., Chen, Q., Yang, H., Sajjad, S.D., Liu, Z., and Masel, I.R. (2017). Sustainion Imidazolium-Functionalized Polymers for Carbon Dioxide Electrolysis. Energy Tech. *5*, 929–936. https://doi.org/10.1002/ente.201600636.

18. Van Der Stam, W. (2023). The Necessity for Multiscale *In Situ* Characterization of Tailored Electrocatalyst Nanoparticle Stability. Chem. Mater. *35*, 386–394. https://doi.org/10.1021/acs.chemmater.2c03286.

19. Lees, E.W., Bui, J.C., Romiluyi, O., Bell, A.T., and Weber, A.Z. (2024). Exploring CO2 reduction and crossover in membrane electrode assemblies. Nat. Chem. Eng. *1*, 340–353. https://doi.org/10.1038/s44286-024-00062-0.

20. Salvatore, D.A., Gabardo, C.M., Reyes, A., O'Brien, C.P., Holdcroft, S., Pintauro, P., Bahar, B., Hickner, M., Bae, C., Sinton, D., et al. (2021). Designing anion exchange membranes for CO2 electrolysers. Nat. Energy *6*, 339–348. https://doi.org/10.1038/s41560-020-00761-x.

21. Lee, D.U., Joensen, B., Jenny, J., Ehlinger, V.M., Lee, S.-W., Abiose, K., Xu, Y., Sarkar, A., Lin, T.Y., Hahn, C., and Jaramillo, T.F. (2023). Controlling Mass Transport in Direct Carbon Dioxide Zero-Gap Electrolyzers via Cell Compression. ACS Sustain. Chem. Eng. *11*, 16661–16668. https://doi.org/10.1021/acssuschemeng.3c05494.

22. Subramanian, S., Yang, K., Li, M., Sassenburg, M., Abdinejad, M., Irtem, E., Middelkoop, J., and Burdyny, T. (2023). Geometric Catalyst Utilization in Zero-Gap CO2 Electrolyzers. ACS Energy Lett. *8*, 222–229. https://doi.org/10.1021/acsenergylett.2c02194.

23. Burdyny, T., Subramanian, S., Kok, J., Gholkar, P., Kumar, A.S., Montfort, H.P.I.v., Kortlever, R., Urakawa, A., and Dam, B. (2024). CO residence time modulates multi-carbon formation rates in a zero-gap Cu based CO2 electrolyzer. Energy Environ Sci. *17*, 6728–6738. https://doi.org/10.21203/rs.3.rs-3535552/v1.

24. Simonson, H., Klein, W.E., Henckel, D., Verma, S., Neyerlin, K.C., and Smith, W.A. (2023). Direct Measurement of Electrochemical Selectivity Gradients over a 25 cm^2 Copper Gas Diffusion Electrode. ACS Energy Lett. *8*, 3811–3819. https://doi.org/10.1021/acsenergylett.3c01489.

25. Zhang, B., Wang, L., Li, D., Li, Z., Bu, R., and Lu, Y. (2022). Tandem strategy for electrochemical CO2 reduction reaction. Chem Catal. *2*, 3395–3429. https://doi.org/10.1016/j.checat.2022.10.017.

26. Zhang, T., Li, Z., Zhang, J., and Wu, J. (2020). Enhance CO2-to-C2+ products yield through spatial management of CO transport in Cu/ZnO tandem electrodes. J. Catal. *387*, 163–169. https://doi.org/10.1016/j.jcat.2020.05.002.

27. Morales-Guio, C.G., Cave, E.R., Nitopi, S.A., Feaster, J.T., Wang, L., Kuhl, K.P., Jackson, A., Johnson, N.C., Abram, D.N., Hatsukade, T., et al. (2018). Improved CO2 reduction activity towards C2+ alcohols on a tandem gold on copper electrocatalyst. Nat. Catal. *1*, 764–771. https://doi.org/10.1038/s41929-018-0139-9.

28. Zhang, T., Bui, J.C., Li, Z., Bell, A.T., Weber, A.Z., and Wu, J. (2022). Highly selective and productive reduction of carbon dioxide to multicarbon products via in situ CO management using segmented tandem electrodes. Nat. Catal. *5*, 202–211. https://doi.org/10.1038/s41929-022-00751-0.

29. Wheeler, D.G., Mowbray, B.A.W., Reyes, A., Habibzadeh, F., He, J., and Berlinguette, C.P. (2020). Quantification of water transport in a CO_2 electrolyzer. Energy Environ. Sci. *13*, 5126–5134. https://doi.org/10.1039/D0EE02219E.

30. Choi, W., Park, S., Jung, W., Won, D.H., Na, J., and Hwang, Y.J. (2022). Origin of Hydrogen Incorporated into Ethylene during Electrochemical CO_2 Reduction in Membrane Electrode Assembly. ACS Energy Lett. *7*, 939–945. https://doi.org/10.1021/acsenergylett.1c02658.

31. Disch, J., Bohn, L., Koch, S., Schulz, M., Han, Y., Tengattini, A., Helfen, L., Breitwieser, M., and Vierrath, S. (2022). High-resolution neutron imaging of salt precipitation and water transport in zero-gap CO2 electrolysis. Nat. Commun. *13*, 6099. https://doi.org/10.1038/s41467-022-33694-y.

32. Huang, Y., Handoko, A.D., Hirunsit, P., and Yeo, B.S. (2017). Electrochemical Reduction of CO_2 Using Copper Single-Crystal Surfaces: Effects of CO* Coverage on the Selective Formation of Ethylene. ACS Catal. *7*, 1749–1756. https://doi.org/10.1021/acscatal.6b03147.

33. Sandberg, R.B., Montoya, J.H., Chan, K., and Nørskov, J.K. (2016). CO-CO coupling on Cu facets: Coverage, strain and field effects. Surf. Sci. *654*, 56–62. https://doi.org/10.1016/j.susc.2016.08.006.

34. Hursán, D., and Janáky, C. (2023). *Operando* characterization of continuous flow CO_2 electrolyzers: current status and future prospects. Chem. Commun. *59*, 1395–1414. https://doi.org/10.1039/D2CC06065E.

35. Moss, A.B., Garg, S., Mirolo, M., Giron Rodriguez, C.A., Ilvonen, R., Chorkendorff, I., Drnec, J., and Seger, B. (2023). In operando investigations of oscillatory water and carbonate effects in MEA-based CO2 electrolysis devices. Joule *7*, 350–365. https://doi.org/10.1016/j.joule.2023.01.013.

36. Garg, S., Xu, Q., Moss, A.B., Mirolo, M., Deng, W., Chorkendorff, I., Drnec, J., and Seger, B. (2023). How alkali cations affect salt precipitation and CO_2 electrolysis performance in membrane electrode assembly electrolyzers. Energy Environ. Sci. *16*, 1631–1643. https://doi.org/10.1039/D2EE03725D.

37. Disch, J., Bohn, L., Metzler, L., and Vierrath, S. (2023). Strategies for the mitigation of salt precipitation in zero-gap CO_2 electrolyzers producing CO. J. Mater. Chem. A *11*, 7344–7357. https://doi.org/10.1039/D2TA09966G.

38. Iglesias van Montfort, H.-P., Li, M., Irtem, E., Abdinejad, M., Wu, Y., Pal, S.K., Sassenburg, M., Ripepi, D., Subramanian, S., Biemolt, J., et al. (2023). Non-invasive current collectors for improved current-density distribution during CO2 electrolysis on super-hydrophobic electrodes. Nat. Commun. *14*, 6579. https://doi.org/10.1038/s41467-023-42348-6.

39. Moore, T., Xia, X., Baker, S.E., Duoss, E.B., and Beck, V.A. (2021). Elucidating Mass Transport Regimes in Gas Diffusion Electrodes for CO_2 Electroreduction. ACS Energy Lett. *6*, 3600–3606. https://doi.org/10.1021/acsenergylett.1c01513.

40. Burdyny, T., and Smith, W.A. (2019). CO2 reduction on gas-diffusion electrodes and why catalytic performance must be assessed at commercially-relevant conditions. Energy Environ. Sci. *12*, 1442–1453. https://doi.org/10.1039/c8ee03134g.

41. Raciti, D., Mao, M., and Wang, C. (2018). Mass transport modelling for the electroreduction of CO_2 on Cu nanowires. Nanotechnology *29*, 044001. https://doi.org/10.1088/1361-6528/aa9bd7.

42. Lu, X., Zhu, C., Wu, Z., Xuan, J., Francisco, J.S., and Wang, H. (2020). In Situ Observation of the pH Gradient near the Gas Diffusion Electrode of CO_2 Reduction in Alkaline Electrolyte. J. Am. Chem. Soc. *142*, 15438–15444. https://doi.org/10.1021/jacs.0c06779.

43. Böhme, A., Bui, J.C., Fenwick, A.Q., Bhide, R., Feltenberger, C.N., Welch, A.J., King, A.J., Bell, A.T., Weber, A.Z., Ardo, S., and Atwater, H.A. (2023). Direct observation of the local microenvironment in inhomogeneous CO_2 reduction gas diffusion electrodes *via* versatile pOH imaging. Energy Environ. Sci. *16*, 1783–1795. https://doi.org/10.1039/D2EE02607D.

44. Iglesias van Montfort, H.-P., and Burdyny, T. (2022). Mapping Spatial and Temporal Electrochemical Activity of Water and CO2 Electrolysis on Gas-Diffusion Electrodes Using Infrared Thermography. ACS Energy Lett. *7*, 2410–2419. https://doi.org/10.1021/acsenergylett.2c00984.

45. Nesbitt, N.T., Burdyny, T., Simonson, H., Salvatore, D., Bohra, D., Kas, R., and Smith, W.A. (2020). Liquid-Solid Boundaries Dominate Activity of CO2Reduction on Gas-Diffusion Electrodes. ACS Catal. *10*, 14093–14106. https://doi.org/10.1021/acscatal.0c03319.

46. Bohra, D., Chaudhry, J.H., Burdyny, T., Pidko, E.A., and Smith, W.A. (2019). Modeling the electrical double layer to understand the reaction environment in a CO2 electrocatalytic system. Energy Environ. Sci. *12*, 3380–3389. https://doi.org/10.1039/c9ee02485a.

47. Rabinowitz, J.A., and Kanan, M.W. (2020). The future of low-temperature carbon dioxide electrolysis depends on solving one basic problem. Nat. Commun. *11*, 5231. https://doi.org/10.1038/s41467-020-19135-8.

48. Dinh, C.T., Burdyny, T., Kibria, M.G., Seifitokaldani, A., Gabardo, C.M., García de Arquer, F.P., Kiani, A., Edwards, J.P., De Luna, P., Bushuyev, O.S., et al. (2018). CO2 electroreduction to ethylene via hydroxide-mediated copper catalysis at an abrupt interface. Science *360*, 783–787. https://doi.org/10.1126/science.aas9100.

49. García de Arquer, F.P., Dinh, C.T., Ozden, A., Wicks, J., McCallum, C., Kirmani, A.R., Nam, D.H., Gabardo, C., Seifitokaldani, A., Wang, X., et al. (2020). CO2 electrolysis to multicarbon products at activities greater than 1 A cm−2. Science *367*, 661–666. https://doi.org/10.1126/science.aay4217.

50. Gu, Z., Shen, H., Chen, Z., Yang, Y., Yang, C., Ji, Y., Wang, Y., Zhu, C., Liu, J., Li, J., et al. (2021). Efficient Electrocatalytic CO2 Reduction to C2+ Alcohols at Defect-Site-Rich Cu Surface. Joule *5*, 429–440. https://doi.org/10.1016/j.joule.2020.12.011.

51. Wang, Y., Shen, H., Livi, K.J.T., Raciti, D., Zong, H., Gregg, J., Onadeko, M., Wan, Y., Watson, A., and Wang, C. (2019). Copper Nanocubes for CO_2 Reduction in Gas Diffusion Electrodes. Nano Lett. *19*, 8461–8468. https://doi.org/10.1021/acs.nanolett.9b02748.

52. Wu, Q., Du, R., Wang, P., Waterhouse, G.I.N., Li, J., Qiu, Y., Yan, K., Zhao, Y., Zhao, W.-W., Tsai, H.-J., et al. (2023). Nanograin-Boundary-Abundant Cu_2O-Cu Nanocubes with High C_{2+} Selectivity and Good Stability during Electrochemical CO_2 Reduction at a Current Density of 500 mA/cm^2. ACS Nano *17*, 12884–12894. https://doi.org/10.1021/acsnano.3c04951.

53. Ma, W., Xie, S., Liu, T., Fan, Q., Ye, J., Sun, F., Jiang, Z., Zhang, Q., Cheng, J., and Wang, Y. (2020). Electrocatalytic reduction of CO2 to ethylene and ethanol through hydrogen-assisted C–C coupling over fluorine-modified copper. Nat. Catal. *3*, 478–487. https://doi.org/10.1038/s41929-020-0450-0.

54. Zheng, M., Wang, P., Zhi, X., Yang, K., Jiao, Y., Duan, J., Zheng, Y., and Qiao, S.-Z. (2022). Electrocatalytic CO_2-to-C_{2+} with Ampere-Level Current on Heteroatom-Engineered Copper *via* Tuning *CO Intermediate Coverage. J. Am. Chem. Soc. *144*, 14936–14944. https://doi.org/10.1021/jacs.2c06820.

55. Zhang, G., Zhao, Z.-J., Cheng, D., Li, H., Yu, J., Wang, Q., Gao, H., Guo, J., Wang, H., Ozin, G.A., et al. (2021). Efficient CO2 electroreduction on facet-selective copper films with high conversion rate. Nat. Commun. *12*, 5745. https://doi.org/10.1038/s41467-021-26053-w.

56. Wang, X., Wang, Z., García de Arquer, F.P., Dinh, C.-T., Ozden, A., Li, Y.C., Nam, D.-H., Li, J., Liu, Y.-S., Wicks, J., et al. (2020). Efficient electrically powered CO2-to-ethanol via suppression of deoxygenation. Nat. Energy *5*, 478–486. https://doi.org/10.1038/s41560-020-0607-8.

57. Fan, M., Huang, J.E., Miao, R.K., Mao, Y., Ou, P., Li, F., Li, X.-Y., Cao, Y., Zhang, Z., Zhang, J., et al. (2023). Cationic-group-functionalized electrocatalysts enable stable acidic CO2 electrolysis. Nat. Catal. *6*, 763–772. https://doi.org/10.1038/s41929-023-01003-5.

58. Kormányos, A., Endrődi, B., Zhang, Z., Samu, A., Mérai, L., Samu, G.F., Janovák, L., and Janáky, C. (2023). Local hydrophobicity allows high-performance electrochemical carbon monoxide reduction to C_{2+} products. EES Catal. *1*, 263–273. https://doi.org/10.1039/D3EY00006K.

59. Li, H., Liu, T., Wei, P., Lin, L., Gao, D., Wang, G., and Bao, X. (2021). High-Rate CO_2 Electroreduction to C_{2+} Products over a Copper-Copper Iodide Catalyst. Angew. Chem. *133*, 14450–14454. https://doi.org/10.1002/ange.202102657.

60. Li, J., Ozden, A., Wan, M., Hu, Y., Li, F., Wang, Y., Zamani, R.R., Ren, D., Wang, Z., Xu, Y., et al. (2021). Silica-copper catalyst interfaces enable carbon-carbon coupling towards ethylene electrosynthesis. Nat. Commun. *12*, 2808. https://doi.org/10.1038/s41467-021-23023-0.

61. Ozden, A., Li, F., Garcıa De Arquer, F.P., Rosas-Hernández, A., Thevenon, A., Wang, Y., Hung, S.-F., Wang, X., Chen, B., Li, J., et al. (2020). High-Rate and Efficient Ethylene Electrosynthesis Using a Catalyst/Promoter/Transport Layer. ACS Energy Lett. *5*, 2811–2818. https://doi.org/10.1021/acsenergylett.0c01266.

62. Ma, Z., Yang, Z., Lai, W., Wang, Q., Qiao, Y., Tao, H., Lian, C., Liu, M., Ma, C., Pan, A., and Huang, H. (2022). CO2 electroreduction to multicarbon products in strongly acidic electrolyte via synergistically modulating the local microenvironment. Nat. Commun. *13*, 7596. https://doi.org/10.1038/s41467-022-35415-x.

63. De Gregorio, G.L., Burdyny, T., Loiudice, A., Iyengar, P., Smith, W.A., and Buonsanti, R. (2020). Facet-Dependent Selectivity of Cu Catalysts in Electrochemical CO_2 Reduction at Commercially Viable Current Densities. ACS Catal. *10*, 4854–4862. https://doi.org/10.1021/acscatal.0c00297.

64. Popović, S., Smiljanić, M., Jovanovič, P., Vavra, J., Buonsanti, R., and Hodnik, N. (2020). Stability and Degradation Mechanisms of Copper-Based Catalysts for Electrochemical CO_2 Reduction. Angew. Chem. *132*, 14844–14854. https://doi.org/10.1002/ange.202000617.

65. Wiesenburg, D.A., and Guinasso, N.L. (1979). Equilibrium solubilities of methane, carbon monoxide, and hydrogen in water and sea water. J. Chem. Eng. Data *24*, 356–360. https://doi.org/10.1021/je60083a006.

66. Weisenberger, S., and Schumpe, A. (1996). Estimation of gas solubilities in salt solutions at temperatures from 273 K to 363 K. AIChE J. *42*, 298–300. https://doi.org/10.1002/aic.690420130.

67. Tan, Y.C., Lee, K.B., Song, H., and Oh, J. (2020). Modulating Local CO2 Concentration as a General Strategy for Enhancing C−C Coupling in CO2 Electroreduction. Joule *4*, 1104–1120. https://doi.org/10.1016/j.joule.2020.03.013.

68. Wang, X., de Araújo, J.F., Ju, W., Bagger, A., Schmies, H., Kühl, S., Rossmeisl, J., and Strasser, P. (2019). Mechanistic reaction pathways of enhanced ethylene yields during electroreduction of CO2–CO co-feeds on Cu and Cu-tandem electrocatalysts. Nat. Nanotechnol. *14*, 1063–1070. https://doi.org/10.1038/s41565-019-0551-6.

69. Henckel, D.A., Counihan, M.J., Holmes, H.E., Chen, X., Nwabara, U.O., Verma, S., Rodríguez-López, J., Kenis, P.J.A., and Gewirth, A.A. (2021). Potential Dependence of the Local pH in a CO_2 Reduction Electrolyzer. ACS Catal. *11*, 255–263. https://doi.org/10.1021/acscatal.0c04297.

70. Lu, X., Zhou, C., Delima, R.S., Lees, E.W., Soni, A., Dvorak, D.J., Ren, S., Ji, T., Bahi, A., Ko, F., and Berlinguette, C.P. (2024). Visualization of CO2 electrolysis using optical coherence tomography. Nat. Chem. *16*, 979–987. https://doi.org/10.1038/s41557-024-01465-5.

71. Ko, Y.-J., Lim, C., Jin, J., Kim, M.G., Lee, J.Y., Seong, T.-Y., Lee, K.-Y., Min, B.K., Choi, J.-Y., Noh, T., et al. (2024). Extrinsic hydrophobicity-controlled silver nanoparticles as efficient and stable catalysts for CO2 electrolysis. Nat. Commun. *15*, 3356. https://doi.org/10.1038/s41467-024-47490-3.

72. O'Brien, C.P., McLaughlin, D., Böhm, T., Xiao, Y.C., Edwards, J.P., Gabardo, C.M., Bierling, M., Wicks, J., Sedighian Rasouli, A., Abed, J., et al. (2024). Scalability and stability in CO2 reduction via tomography-guided system design. Joule *8*, 2903–2919. https://doi.org/10.1016/j.joule.2024.07.004.

73. Niblett, D., Mularczyk, A., Niasar, V., Eller, J., and Holmes, S. (2020). Two-phase flow dynamics in a gas diffusion layer - gas channel - microporous layer system. J. Power Sources *471*, 228427. https://doi.org/10.1016/j.jpowsour.2020.228427.

74. Schmidt, G., Niblett, D., Niasar, V., and Neuweiler, I. (2024). Modeling of Pore-Scale Capillary-Dominated Flow and Bubble Detachment in PEM Water Electrolyzer Anodes Using the Volume of Fluid Method. J. Electrochem. Soc. *171*, 074503. https://doi.org/10.1149/1945-7111/ad5708.

75. Dubau, L., Castanheira, L., Chatenet, M., Maillard, F., Dillet, J., Maranzana, G., Abbou, S., Lottin, O., De Moor, G., El Kaddouri, A., et al. (2014). Carbon corrosion induced by membrane failure: The weak link of PEMFC long-term performance. Int. J. Hydrogen Energy *39*, 21902–21914. https://doi.org/10.1016/j.ijhydene.2014.07.099.

76. Phillips, A., Ulsh, M., Porter, J., and Bender, G. (2017). Utilizing a Segmented Fuel Cell to Study the Effects of Electrode Coating Irregularities on PEM Fuel Cell Initial Performance. Fuel Cell. *17*, 288–298. https://doi.org/10.1002/fuce.201600214.

77. Phillips, A., Ulsh, M., Neyerlin, K.C., Porter, J., and Bender, G. (2018). Impacts of electrode coating irregularities on polymer electrolyte membrane fuel cell lifetime using quasi in-situ infrared thermography and accelerated stress testing. Int. J. Hydrogen Energy *43*, 6390–6399. https://doi.org/10.1016/j.ijhydene.2018.02.050.

78. Yang, K., Kas, R., Smith, W.A., and Burdyny, T. (2021). Role of the Carbon-Based Gas Diffusion Layer on Flooding in a Gas Diffusion Electrode Cell for Electrochemical CO_2 Reduction. ACS Energy Lett. *6*, 33–40. https://doi.org/10.1021/acsenergylett.0c02184.

79. Perego, M., Oldani, D., and Ottaviani, A. (2013). US Patent 8372255: Elastic Current Collector for Electrochemical Cells.

80. Rufer, S., Nitzsche, M., Garimella, S., Lake, J., and Varanasi, K.K. (2023). Hierarchically Conductive Electrodes Unlock Stable and Scalable CO2 Electrolysis. Preprint at ChemRxiv. https://doi.org/10.26434/chemrxiv-2023-c2zz0.

81. Filippi, M., Möller, T., Pastusiak, R., Magori, E., Paul, B., and Strasser, P. (2024). Scale-Up of PTFE-Based Gas Diffusion Electrodes Using an Electrolyte-Integrated Polymer-Coated Current Collector Approach. ACS Energy Lett. *9*, 1361–1368. https://doi.org/10.1021/acsenergylett.4c00114.

82. Lin, R., Sander, H., Gülzow, E., and Friedrich, A. (2010). Investigation of Locally Resolved Current Density Distribution of Segmented PEM Fuel Cells to Detect Malfunctions. ECS Trans. *26*, 229–236. https://doi.org/10.1149/1.3428993.

83. Biswas, I., Sánchez, D.G., Schulze, M., Mitzel, J., Kimmel, B., Gago, A.S., Gazdzicki, P., and Friedrich, K.A. (2020). Advancement of Segmented Cell Technology in Low Temperature Hydrogen Technologies. Energies *13*, 2301. https://doi.org/10.3390/en13092301.

84. Osmieri, L., Mauger, S., Ulsh, M., Neyerlin, K.C., and Bender, G. (2020). Use of a segmented cell for the combinatorial development of platinum group metal-free electrodes for polymer electrolyte fuel cells. J. Power Sources *452*, 227829. https://doi.org/10.1016/j.jpowsour.2020.227829.

85. Reshetenko, T.V., Bender, G., Bethune, K., and Rocheleau, R. (2013). A segmented cell approach for studying the effects of serpentine flow field parameters on PEMFC current distribution. Electrochim. Acta *88*, 571–579. https://doi.org/10.1016/j.electacta.2012.10.103.

86. Chen, G., Zhu, Y., She, S., Lin, Z., Sun, H., and Huang, H. (2024). Component leaching of water oxidation electrocatalysts. InfoMat *6*, e12609. https://doi.org/10.1002/inf2.12609.